originally in the $1a_2''$ orbital are transferred to the $2a_1'$ orbital where they support metal-metal bonding, and the $1a_2''$ orbital then accepts charge density from the ligands to form metal-ligand bonds.

In Table XIV we list the Mulliken populations of the canonical metal cluster orbitals for the intermediate "compounds" and for the entire molecules. It can be seen that in the six-electron systems both $1a_2''$ and $2a_1'$ orbitals accept a certain amount of charge from the ligands but the $2a_1'$ orbital is less populated. For the eight-electron systems the situation is quite different. Compared with the six-electron systems, the population in the $1a_2''$ orbital does not change significantly, even though it is fully occupied in $[Nb_3]^{7+}$. However the population in the $2a_1'$ orbital has been tremendously increased. Since the populations in other high orbitals are not greatly changed from the six-electron systems to the eight-electron systems, the $2a_1'$ orbital should owe its high charge population to the electrons originally occupying the $1a_2''$ orbital in $[Nb_3]^{7+}$.

One may also notice that the metal-metal bonding orbitals in $[Nb_3Cl_{10}(PH_3)_3]^-$ are not "purely" contributed by the niobium atoms (see Table XII). Both $13a_1$ and 18e orbitals have nonnegligible contributions from the terminal chlorine ligands, so that the metal-metal bonding is "perturbed". However, the contributions of the terminal chlorine atoms to the 19a and 18e orbitals are significantly decreased in $Nb_3Cl_7(PH_3)_6$, mainly because the molecule has fewer terminal chlorine atoms. This may be an indication that in some cases the terminal ligands may influence the metal-metal bond strength or may change the bonding scheme in molecules of this type.

Concluding Remarks. It has now been demonstrated that triniobium chloro/phosphine cluster compounds closely similar to the $Nb_3Cl_4Cl_{3/3}Cl_{6/2}$ subunits in Nb_3Cl_8 can be made, as well as a similar tantalum compound (although Ta_3Cl_8 is unknown). It is interesting that the cluster electron counts for our discrete species (six, eight) bracket that for the subunit in Nb_3Cl_8 (seven). It should be noted that we do not believe that the Nb-Nb distance in Nb_3Cl_8 should be compared with those found in the discrete clusters because constraints specific to the extended array may have a strong influence on this. However, the two discrete species can reasonably be compared with each other, and the relationship between them is satisfactorily explained by the molecular orbital calculations. These calculations show that there are six M-M bonding electrons in the six-electron system and eight in the eight-electron system, whereas in earlier work it appeared that the role of the last two electrons of an eight-electron system containing molybdenum atoms might be nonbonding or even slightly antibonding.

Acknowledgment. We are grateful to the Robert A. Welch Foundation for support (Grant No. A-494).

Supplementary Material Available: Full listings of bond distances and bond angles and anisotropic displacement parameters for the crystal structures of $Nb_3Cl_7(PMe_2Ph)_6{\cdot}C_7H_8$, $HPEt_3[Nb_3Cl_{10}(pEt_3)]{\cdot}1.25C_7H_8$, and its Ta analogue (20 pages); tables of observed and calculated structure factors for all three structures (78 pages). Ordering information is given on any current masthead page.

Notes

Contribution from the Department of Chemistry and Biochemistry, University of California, Los Angeles, California 90024-1569

Angular-Overlap Interpretation of σ and π Bonding of PF_3 and PCl_3 in $PtCl_3L^-$ Complexes

Huey-Rong Jaw and Jeffrey I. Zink*

Received March 4, 1988

The determination of the magnitudes of σ and π interactions of trihalophosphine ligands with transition metals has attracted widespread interest. The PF_3 ligand is generally considered to be similar to CO in its properties, but direct comparison of the individual σ and π components with those of other ligands is scarce.

The most insight into the σ and π properties has been obtained from vibrational spectroscopic studies of substituted metal carbonyl compounds.[1] The common lists of π acceptor ligand series have been derived from trends in carbonyl stretching frequencies.[1,3] For the trihalophosphine ligands and comparison ligands to be treated in this paper, the σ donor trend is $P(n\text{-}Bu)_3 > PF_3 \approx PCl_3 > CO$ and the π acceptor trend is $PF_3 > CO > PCl_3 > P(n\text{-}Bu)_3$. Additional insight into the relative σ and π properties has been provided by UV-PES,[4-6] molecular orbital theoretical studies,[7,8] and mass spectroscopic studies.[9,10]

Another experimental method of determining the σ and π interactions of ligands with transition metals is electronic absorption spectroscopy. The σ and π interactions can be determined from the d-d transition energies and interpreted by using the angular-overlap theory.[11,12] A series of compounds that is proving to be amenable to detailed study is the $PtCl_3L^{n-}$ series, where L can range from "Werner" ligands[13-21] to ligands of organometallic interest such as olefins,[22,23] phosphines,[24,25] CO,[26] carbenes, and acetylenes. Only the ligand L is changed in this series. Hence, systematic changes in the σ and π properties can be interpreted from analysis of the electronic spectra.

We report here electronic spectroscopic results for $(Pr_4N)[PtCl_3PF_3]$ and $(Pr_4N)[PtCl_3PCl_3]$. The spectra are analyzed by using the angular-overlap theory, and the σ and π interaction parameters are determined. The σ and π properties of PF_3 and

(1) Graham, W. A. G. *Inorg. Chem.* **1968**, *7*, 315.
(2) (a) Cotton, F. A.; Wilkinson, G. *Advanced Inorganic Chemistry*; Wiley: New York, 1980; p 1078. (b) Huheey, J. E. *Inorganic Chemistry*; Harper and Row: New York, 1983; p 432.
(3) Timney, J. A. *Inorg. Chem.* **1979**, *18*, 2502.
(4) Yarbrough, L. W.; Hall M. B. *Inorg. Chem.* **1978**, *17*, 2269.
(5) Avanzino, S. C.; Chen, H.-W.; Donahue, C. J.; Jolly, W. L. *Inorg. Chem.* **1980**, *19*, 2201.
(6) Daamen, H.; Boxhoorn, G.; Oskam, A. *Inorg. Chim. Acta* **1978**, *28*, 263.
(7) Ziegler, T.; Rauk, A. *Inorg. Chem.* **1979**, *18*, 1755.
(8) Xiao, S.-X.; Trogler, W. C.; Ellis, D. E.; Berkovitch-Yellin, Z. *J. Am. Chem. Soc.* **1983**, *105*, 7033.
(9) Saalfeld, F. E.; Mcdowell, M. V.; Gondal, S. K.; Macdiarmid, A. G. *J. Am. Chem. Soc.* **1968**, *90*, 3684.
(10) Hitchcock, P. B.; Jacobson, B.; Pidock, A. *J. Chem. Soc., Dalton Trans.* **1977**, 2043.
(11) Schaffer, C. E.; Jørgensen, C. K. *Mol. Phys.* **1965**, *9*, 401.
(12) Schaffer, C. E. *Struct. Bonding (Berlin)* **1968**, *5*, 68.
(13) Fenske, R. F.; Martin, D. S.; Ruedenberg, K. *Inorg. Chem.* **1962**, *1*, 441.
(14) (a) Kroening, R. F.; Rush, R. M.; Martin, D. S.; Clardy, J. C. *Inorg. Chem.* **1974**, *13*, 1366. (b) Martin, D. S.; Tucker, M. A.; Kassman, A. J. *Inorg. Chem.* **1965**, *4*, 1682.
(15) Fanwick, P. E.; Martin, D. S. *Inorg. Chem.* **1973**, *12*, 24.
(16) Martin, D. S. *Inorg.* Chim. *Acta, Rev.* **1971**, *5*, 107.
(17) Patterson, H. H.; Godfrey, J. J.; Khan, S. M. *Inorg. Chem.* **1972**, *11*, 2872.
(18) Francke, E.; Moncuit, C. *Theor.* Chim. Acta **1973**, *29*, 319.
(19) Tuszynski, W.; Gliemann, G. *Z. Naturforsch., A: Phys., Phys. Chem., Kosmophys.* **1979**, *34A*, 211.
(20) Vanquickenborne, L. G.; Ceulemans, A. *Inorg. Chem.* **1981**, *20*, 796.
(21) Chang, T.-H.; Zink, J. I. *Inorg. Chem.* **1985**, *24*, 4499.
(22) Chang, T.-H.; Zink J. I. *J. Am. Chem. Soc.* **1984**, *106*, 287.
(23) Jaw, H.-*R.*; Chang, T.-H.; Zink, J. I *Inorg. Chem.* **1987**, *26*, 4204.
(24) Philips, J.; Zink, J. I. *Inorg. Chem.* **1986**, *25*, 103.
(25) Chang, T.-H.; Zink, J. I. *Inorg. Chem.* **1986**, *25*, 2736.
(26) Chang, T.-H.; Zink, J. I. *J. Am. Chem. Soc.* **1987**, *109*, 692.

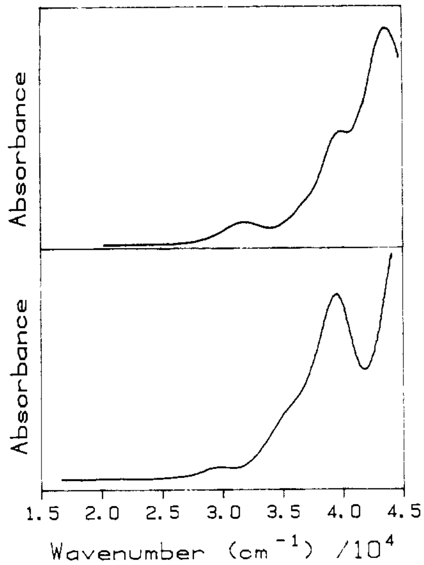

Figure 1. Electronic absorption spectra of $(Pr_4N)[PtCl_3(PF_3)]$ (top) and $(Pr_4N)[PtCl_3(PCl_3)]$ (bottom) in dichloromethane solution at room temperature.

$PtCl_3$ are compared to those of other ligands, and the position of the ligands in the two-dimensional spectrochemical series is determined for the first time.

Experimental Section

The platinum compounds were prepared according to the literature methods, where PX_3 is reacted directly with the *n*-propylammonium salt of the platinum dimer $Pt_2Cl_6^{2-}$.[27,28] The syntheses and manipulations of the compounds $(Pr_4N)[PtCl_3(PX_3)]$, where X = F and Cl, were conducted under a dry nitrogen atmosphere. Both PF_3 and PCl_3 are toxic and moisture-sensitive. PF_3 was purified by passing it through two ethyl acetate slush traps (−83.6 °C). PCl_3 was used without further purification. Methylene chloride was distilled from calcium hydride and was deoxygenated before use.

Single crystals of $(Pr_4N)[PtCl_3(PF_3)]$ were grown between quartz plates from a methylene solution chloride under a dry N_2 atmosphere. A drop of the sample solution was placed on top of one quartz plate by using a syringe, and the second quartz plate was pressed onto the first. The quartz plates were placed in a bell jar, which was connected to a nitrogen line. A small beaker of methylene chloride was also placed in the bell jar. The bell jar was evacuated, and nitrogen was flushed back in so that the atmosphere consisted of solvent-saturated nitrogen. By use of this method, slow crystallization occurred and well-formed rectangular crystals were obtained. Crystals that had a first-order gray color and distinct extinction axes when examined under the polarizing microscope were chosen for study. Attempts to grow single crystals of $(Pr_4N)[PtCl_3(PCl_3)]$ suitable for optical study were unsuccessful.

The single-crystal polarized absorption spectra were measured by using the instrument described previously.[22] The spectra labeled as "parallel" were taken with the polarization direction along the extinction axis parallel to the long crystal axis. The spectra labeled "perpendicular" were obtained in the orthogonal extinction direction. Because the crystal structure is not known, these labels refer to the macroscopic extinction axes and do not refer to the molecular axes. The calculations were carried out by diagonalizing the ligand field matrix including spin–orbit coupling as described previously.[18,26]

Results

1. $(Pr_4N)[PtCl_3(PF_3)]$. The solution spectrum of $(Pr_4N)[PtCl_3(PF_3)]$ in dichloromethane, shown in Figure 1, contains three bands at 31 750, 39 840, and 42 920 cm^{-1} with extinction coefficients of 570, 2500, and 4700 M^{-1} cm^{-1}, respectively. The band at 31 750 cm^{-1} is broader than the others. It has a long tail on the low-energy side. The band at 39 480 cm^{-1} is on a steep, fast-rising slope. In addition to the three well-defined peaks, a weak shoulder is apparent at about 36 000 cm^{-1}.

(27) Crocker, C.; Goggin, P. L.; Goodfellow, R. J. *J. Chem. Soc., Dalton Trans.* **1976**, 2494.
(28) Goggin, P. L.; Goodfellow, R. J.; Reed, F. J. S. *J. Chem. Soc., Dalton Trans.* **1972**, 1298.

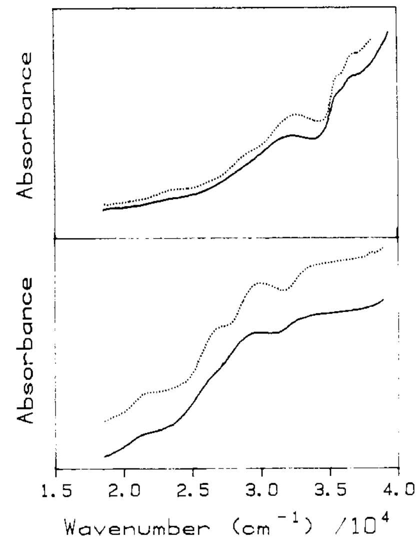

Figure 2. Electronic absorption spectra of $(Pr_4N)[PtCl_3(PF_3)]$ (top) and $(Pr_4N)[PtCl_3(PCl_3)]$ (bottom) in Nujol mulls. The room-temperature spectra are shown by the solid lines, and the 77 K spectra are shown by the dotted lines.

Table I. Absorption Band Maxima of $(Pr_4N)[PtCl_3(PF_3)]$ and $(Pr_4N)[PtCl_3(PCl_3)]$ (cm^{-1})

		mull		cryst	
bands	soln room temp	77 K	room temp	10 K	room temp
		$[PtCl_3(PF_3)]^-$			
	42 920 (4700)[a]		43 500[b]		
$^1B_2$	39 840 (2500)		39 400		
$^1A_2$	36 000[b] (800)	36 200	36 000	37 100	36 500[b]
$^1B_1$	31 750 (570)	32 300	31 750	33 300	32 500
		28 700	28 000	29 300	29 200
		26 000		25 800	
		23 000	22 000–24 000[c]	23 300	
		$[PtCl_3(PCl_3)]^-$			
	39 530 (4500)[a]				
$^1B_2$	35 000[b] (1800)	37 000[c]	36 000[b]		
$^1A_2$		33 800[c]	33 000[c]		
$^1B_1$	29 670 (500)	29 940	29 760		
		26 700	26 000		
		22 900–24 100	21 000–23 000		
		21 600			

[a] The numbers in parentheses are the extinction coefficients in M^{-1} cm^{-1}. [b] Observed as a shoulder in the spectrum. [c] Unresolved bands.

The Nujol mull spectra of $(Pr_4N)[PtCl_3(PF_3)]$ are shown in Figure 2. The room-temperature mull spectrum is virtually the same as the solution spectrum except that the band positions shift slightly to higher energy. Three features become more distinct, two weak shoulders that appear at about 36 000 cm^{-1} and a very weak and broad band that appears between 22 000 and 24 000 cm^{-1}. When the Nujol mull sample is cooled to 77 K, all of the bands sharpen and shift toward higher energy. The two weak shoulders become more resolved and have maxima at about 36 760 and 35 580 cm^{-1}. The broad band at 31 750 cm^{-1} resolves into two features, distinct peak at 32 300 cm^{-1} and a shoulder at about 28 700 cm^{-1}. The weak band between 22 000 and 24 000 cm^{-1} becomes more apparent and is centered at about 23 000 cm^{-1}. A new weak feature is observed at about 26 000 cm^{-1}. The positions of all of the bands are summarized in Table I.

The single-crystal polarized electronic absorption spectra of $(Pr_4N)[PtCl_3(PF_3)]$ measured at 10 K are shown in Figure 3. All peaks show a blue shift of several hundred wavenumbers at 10 K relative to those in the mull spectra at 77 K. The electronic absorption spectra consist of five bands in the region between 18 000 and 38 000 cm^{-1}. The lowest energy band, at 23 000 cm^{-1}, is allowed in both polarizations. The distinct but not quite resolved

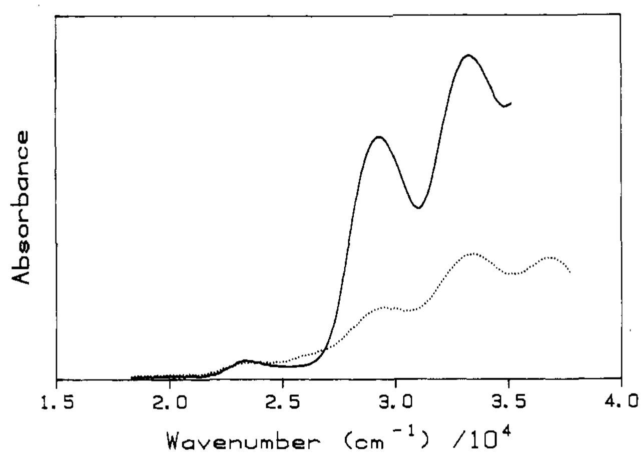

Figure 3. Single-crystal polarized absorption spectra of $(Pr_4N)[PtCl_3(PF_3)]$ taken at 10 K. The spectra shown by the solid line and the dotted line were obtained in orthogonal extinction directions of the microcrystal.

shoulder at 25 800 cm^{-1} has slightly more intensity in the parallel polarization. The third band, more intense in perpendicular polarization, is at 29 300 cm^{-1}. These three bands contribute to the nonzero-intensity tail of the 31 750-cm^{-1} band in the solution and mull spectra. The fourth peak, which occurs at 33 300 cm^{-1}, is allowed in both polarizations but shows greater intensity in the perpendicular polarization. The last band occurs at 37 100 cm^{-1}. It is off scale in perpendicular polarization but is observed in parallel polarization. The intensity of this band decreases with decreasing temperature.

2. $(Pr_4N)[PtCl_3(PCl_3)]$. The methylene chloride solution spectrum, shown in Figure 1, contains two distinct bands at 29 670 and 39 530 cm^{-1}, with extinction coefficients of 500 and 4500 M^{-1} cm^{-1}, respectively. The peak at 29 670 cm^{-1} is broad and unsymmetrical. A shoulder at about 35 000 cm^{-1} is also observed. The Nujol mull spectra are shown in figure 2. In the room-temperature mull spectrum, the broad band that occurred at 29 670 cm^{-1} in solution appears as a combination of a main band at 29 760 cm^{-1} and a shoulder to the low-energy side. In addition, a broad weak band is observed between 21 000 and 23 000 cm^{-1}. All bands become sharper and shift to higher energy at low temperature. The broad band at 29 760 cm^{-1} clearly resolves into a distinct band centered at 29 940 cm^{-1} and a shoulder at 26 700 cm^{-1}. The broad band between 21 000 and 23 000 cm^{-1} becomes more distinct and shifts to about 23 000 cm^{-1}. The positions of all of the bands are summarized in Table I.

Discussion

1. Assignments. The pattern of the spectra of $PtCl_3(PF_3)^-$ and $PtCl_3(PCl_3)^-$ is similar to that of the other $PtCl_3L^{n-}$ compounds that have been studied in our laboratory.[21-25] The pattern consists of two or three bands with extinction coefficients smaller than about 10^2 M^{-1} cm^{-1} on the low-energy side of the spectrum, two or three bands with extinction coefficients between 10^2 and 10^3 M^{-1} cm^{-1} in the middle of the spectrum, and finally high-intensity bands ($\epsilon > 10^3$) in the high-energy region. The d orbitals and the excited states discussed here are based on the same axis system as that in the previous studies.[21-26] The x axis is defined to lie along the unique metal-ligand bond, and the z axis is perpendicular to the square plane. The B_1 irreducible representation is defined as the one symmetrical to reflection in the xy mirror plane.

The absorption data for the $PtCl_3(PF_3)^-$ compound are summarized in Table I. The assignment of the bands in the spectra of $PtCl_3(PF_3)^-$ is based on both the solution and the 10 K single-crystal spectra with the assistance of the 77 K Nujol mull data. The lowest energy spin-allowed d–d transition is assigned to the broad solution band at 31 750 cm^{-1}. This corresponds to the $^1A_1$ to $^1B_1$, d_{xy} to $d_{x^2-y^2}$ transition. This band shifts to 32 300 and 33 300 cm^{-1} as the temperature is decreased to 77 and 10 K, respectively. The shoulder at about 35 000 cm^{-1}, observed from the solution spectrum, is assigned as the $^1A_1$ to $^1A_2$, d_{yz} to $d_{x^2-y^2}$ transition. It shifts to 37 100 cm^{-1} at 10 K. In the corresponding region of the 77 K Nujol mull spectrum, two weak shoulders are observed at 36 760 and 35 580 cm^{-1}. Their band widths at half-height are small compared to those of the d–d bands. Therefore, these two weak shoulders are probably vibronic structure on the $^1A_2$ band. Two bands, those at 39 800 cm^{-1} and at 42 900 cm^{-1}, are on scale only in the solution spectrum. The band at 39 800 cm^{-1} is assigned as the $^1A_1$ to $^1B_2$, d_{xz} to $d_{x^2-y^2}$ transition. The band at 42 900 cm^{-1} could be either the $^1A_1$ to $^1A_1$, d_{z^2} to $d_{x^2-y^2}$ ligand field band or the chloride to platinum charge-transfer transition. The known chloride to platinum charge-transfer band is at 45 300 cm^{-1} in $[PtCl_3(NH_3)]^-$.[15] Bands lower than 30 000 cm^{-1} are assigned to spin-forbidden transitions. Although the 10 K single-crystal spectra show distinct band maxima in the low-energy region, the ligand field calculations including spin-orbit coupling that are discussed below show that these band maxima are actually a superposition of clusters of closely spaced spin–orbit-coupled components of the triplet states. These triplet states are assigned primarily by using the ligand field theory.

Similar assignments are made for the $PtCl_3(PCl_3)^-$ compound. The absorption bands of the PCl_3 complex are lower in energy than those of the PF_3 complex. The lowest energy $^1B_1$ band is at 29 670 cm^{-1} in the room-temperature solution spectra and at 29 940 cm^{-1} in the 77 K Nujol mull spectrum. This band is about 2500 cm^{-1} lower in energy than the corresponding band in the PF_3 complex. The two spin-allowed d–d bands to higher energy are partially obscured by the intense (ϵ = 4500) band at 39 500 cm^{-1}. There is a broad shoulder between 33 000 and 38 000 cm^{-1} in the 77 K mull spectrum, which is probably composed of the partial overlap of the $^1A_2$ and $^1B_2$ bands. If the bandwidths are similar to those in the $PtCl_3(PF_3)^-$ spectrum, the peak maxima of these bands are estimated to be at about 34 000 and 38 000 cm^{-1}, respectively. The highest energy band at 39 500 cm^{-1}, observed only from the solution spectrum, is either the $^1A_1$ band or the chloride to platinum charge-transfer band. Bands lower than 28 000 cm^{-1}, observed from the 77 K Nujol mull spectrum, are again the spin-forbidden transitions.

2. AOM Calculations. The calculations of the transition energies and the AOM σ and π interaction parameters are carried out by using the procedures described previously.[26] The σ and π parameters for the chloride ligands are assumed to be the same for each chloride. These two parameters and the spin–orbit coupling constant are assumed to be transferable between the $[PtCl_3L]^{n-}$ complexes within a small range of several hundred wavenumbers. This range of uncertainties in the parameters arises partly from the inherent uncertainties in the fitting procedure and partly from the fact that the parameters for chloride in the $PtCl_3L^-$ complexes are expected to change slightly as the ligand L is varied.

The transition energies for both $PtCl_3(PF_3)^-$ and $PtCl_3(PCl_3)^-$ were calculated by using fixed values of the σ and π parameters for the chloride ligands and of the spin–orbit coupling constant. The σ and π parameters for the phosphine ligand were varied until the best fit between the observed and calculated energies was obtained. The fixed chloride parameters are identical with those used in the calculations of the $PtCl_3(PEt_3)^-$ complex.[24]

The results of the calculations and the values of the parameters that were used in them are given in Table II. The mean discrepancies between the observed and calculated singlet-state energies are about 400 cm^{-1} for the $PtCl_3(PF_3)^-$ complex and 105 cm^{-1} for the $PtCl_3(PCl_3)^-$ compound. The states that give rise to the calculated transitions are the same as those assigned above. The calculated triplet-state energies form clusters of closely spaced components that are also in good agreement with the observed absorption bands with small molar absorptivities.

It must be noted that the excellent agreement does not constitute proof of the assignment. Other sets of parameters can be used to generate roughly the same transition energies. However, the severe constraints imposed by using fixed chloride parameters and a fixed spin–orbit coupling constant limit the range of parameters to those reported here.

According to the AOM calculations, PF_3 has a σ value of 23 100 ± 900 cm^{-1} and a π value of −1390 ± 800 cm^{-1}. The PCl_3 ligand has a σ value of 21 100 ± 1200 cm^{-1} and a π value of 525 ± 800

Table II. Band Assignments and Calculated Transition Energies for $(Pr_4N)[PtCl_3(PF_3)]$ and $(Pr_4N)[PtCl_3(PCl_3)]$[a]

Pt–PF$_3$ obsd	Pt–PF$_3$ calcd	assgnt	Pt–PCl$_3$ obsd	Pt–PCl$_3$ calcd
		Singlet d–d		
32 300	32 663	$^1B_1$	29 940	30 055
36 200	35 985	$^1A_2$	33 800	33 822
39 900	39 947	$^1B_2$	37 700	37 027
	40 162	$^1A_1$		38 028
		Triplet d–d		
	22 657	B_2		20 480
	22 837	A_1		20 543
23 000	23 048	B_1	21 600	20 934
(22 900–23 800)			(21 050–22 030)	
	24 677	A_2		22 098
	25 789	B_2		23 383
26 000	26 127	B_1	23 540	23 553
(25 600–26 700)			(22 990–24 100)	
	26 177	A_2		23 883
	26 781	A_1		24 414
28 700	28 875	B_2	26 700	26 706
(28 170–29 400)			(25 970–27 030)	
	29 638	A_1		26 851
	30 428	A_2		27 793
	31 650	B_1		29 266

[a] The transition energies for $PtCl_3(PF_3)^-$ were calculated by using the following parameters (cm^{-1}): $l_\sigma^{Cl} = 11\,800$, $l_\pi^{\parallel,Cl} = 3000$, $L_\pi^{\perp,Cl} = 2700$, $l_\sigma^{PF_3} = 22\,900$, $l_\pi^{\parallel,PF_3} = 1020$, $l_\pi^{\perp,PF_3} = -2050$, $B = 630$, $C = 3000$, SOC = 2850, $\sigma_{sd} = 14\,575$. The transition energies for $PtCl_3(PCl_3)^-$ were calculated by using the following parameters (cm^{-1}): $l_\sigma^{Cl} = 11\,800$, $l_\pi^{\parallel,Cl} = 3000$, $l_\pi^{\perp,Cl} = 2700$, $l_\sigma^{PCl_3} = 20\,000$, $l_\pi^{\parallel,PCl_3} = 1450$, $l_\pi^{\perp,PCl_3} = -1150$, $B = 630$, $C = 3000$, SOC = 2850, $\sigma_{sd} = 13\,850$.

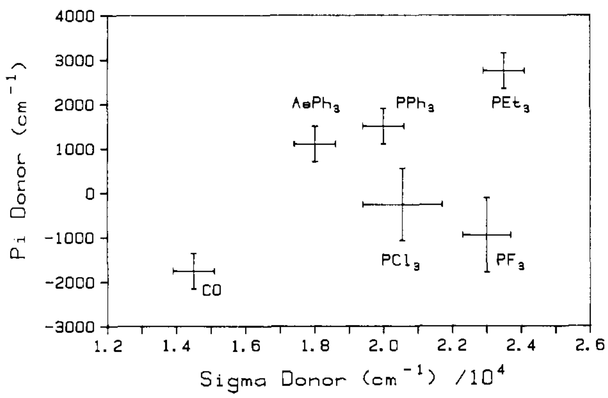

Figure 4. Two-dimensional spectrochemical series for the phosphine ligands and other ligands of interest in organometallic chemistry. The π acceptor strength increases from top to bottom. The σ donor strength increases from left to right.

cm^{-1}. The uncertainties in these values are larger than those in the ligand field parameters obtained from other platinum compounds in which the transition energies could be measured with high accuracy from single-crystal polarized absorption spectra. In addition, the π values are the average of the in-plane and out-of-plane components, which reflect the different magnitudes of π interaction of the ligand with the d_{xy} and the d_{xz} orbitals, respectively. It is important to note that the sign of the π parameter does not have an intrinsic meaning. Only the relative values can be interpreted. These parameters are the result of a complete calculation in which no approximations regarding the π parameters have been made. It has long been known that the AOM π parameter for amines is not zero.[20] When the complete fit to experimental spectra is obtained and the π value for amine is allowed to vary in order to obtain the best fit, the π value is generally greater than zero. Thus, the small positive value of the π parameter for the PCl_3 ligand should be interpreted to mean that the ligand is a poorer π acceptor (or conversely a better π donor) than the PF_3 ligand and a much better π acceptor (or poorer donor) than the chloride ligand. The values of the Racah B and C parameters are a measure of the nephelauxetic effect. Because the variations of these parameters are small compared to the uncertainties, no meaningful comparisons can be made.

The relationship of the ligand field parameters of both PF_3 and PCl_3 to those of other phosphine ligands and ligands of interest in organometallic chemistry are shown in the two-dimensional spectrochemical series in Figure 4. The results show that PF_3 is a surprisingly good σ donor. Its σ donor interaction with platinum is stronger than that of CO, PPh_3, and PCl_3 but weaker than that of PEt_3. The large σ donor interaction is consistent with a large synergistic effect.[2] The π back-bonding ability of PF_3 is stronger than that of any of the other phosphines which have been studied by electronic spectroscopy but slightly weaker than that of CO.

Acknowledgment. We thank the National Science Foundation (Grant CHE 85-09329) for support of this work.

Registry No. $(Pr_4N)[PtCl_3(PF_3)]$, 113258-11-0; $(Pr_4N)[PtCl_3(PCl_3)]$, 113258-12-1; PF_3, 7783-55-3; PCl_3, 7719-12-2.

Contribution from the Research School of Chemistry,
The Australian National University,
G.P.O. Box 4, Canberra, ACT 2601, Australia

Platinum(IV) Cage Chemistry: Crystal Structure of [1,8-Bis(hydroxylamino)-3,6,10,13,16,19-hexaazabicyclo[6.6.6]eicosane]platinum(IV) Trifluoromethanesulfonate Hydrate

Karl S. Hagen,*,† Peter A. Lay, and Alan M. Sargeson*

Received July 28, 1987

We recently reported the synthesis and properties of platinum(IV) cage complexes prepared by the template synthesis about $[Pt(en)_3]^{4+}$.[1] Reaction of $[Pt(en)_3]^{4+}$ with formaldehyde and ammonia resulted in the preparation of $[Pt(sep)]^{4+}$,[1-3] while the use of $CH_2NO_2^-$ as a nucleophile resulted in the preparation of $[Pt((NO_2)_2sar)]^{4+}$.[1-3] On reduction of this complex by $SnCl_2$/HCl, a complex believed to be $[Pt((NH_2)_2sar)]^{4+}$ was formed;[1,3] however, additional work indicated that this complex could be the bis(hydroxylamine) species $[Pt(NHOH)_2sar)]^{4+}$.[4,5] We therefore embarked on a crystallographic analysis of this complex. Such a study was also of interest to determine the coordination geometry about the platinum for comparison with the structure of $[Pt(sep)](S_2O_6)_2\cdot{}^5/_2H_2O$, which has an approximate trigonal-prismatic geometry.[2] It was also necessary to check the identity of the cage complex obtained from the $SnCl_2$/HCl reduction of $[Pt((NO_2)_2sar)]^{4+}$ ion in order to reinterpret the electrochemical and spectroscopic properties of the product, if necessary.

Experimental Section

$[Pt((NHOH)_2sar)]^{4+}$ was prepared by the $SnCl_2$/HCl reduction of $[Pt((NO_2)_2sar)]^{4+}$ [1] and was recrystallized from hot 6 M CF_3SO_3H. After slow cooling to room temperature, the solution was cooled at 4 °C for 2 days, affording colorless crystals of $[Pt((NHOH)_2sar)](CF_3SO_3)_4\cdot H_2O$.[6] X-ray photographs of a crystal mounted on a quartz fiber revealed only $\bar{1}$ Laue symmetry, indicating a triclinic space group. Successful solution and refinement of the structure establishes it to be $P\bar{1}$. The orientation matrix and unit cell dimensions were calculated by least-squares treatment of 25 machine-centered reflections ($24° < 2\theta < 26°$) on a Nicolet R3m four-circle diffractometer using graphite-monochromatized Mo Kα radiation. Crystallographic details are given in Table I. Three check reflection intensities were measured every 100 reflections and exhibited no decay. The data were processed with the program XTAPE of the SHELXTL program package (Nicolet XRD Corp., Madison, WI), and an analytical absorption correction was applied to the data. The positions of the heavy atoms were obtained from a Patterson

† Current address: Department of Chemistry, Emory University, Atlanta, GA 30322.